



**HAL**  
open science

# Robustness of district heating versus electricity-driven energy system at district level: A multi-objective optimization study

Jaume Fitó, Mathieu Vallée, Alain Ruby, Etienne Cuisinier

## ► To cite this version:

Jaume Fitó, Mathieu Vallée, Alain Ruby, Etienne Cuisinier. Robustness of district heating versus electricity-driven energy system at district level: A multi-objective optimization study. *Smart Energy*, 2022, 6, pp.100073. 10.1016/j.segy.2022.100073 . hal-04575419

**HAL Id: hal-04575419**

**<https://hal.science/hal-04575419>**

Submitted on 22 Jul 2024

**HAL** is a multi-disciplinary open access archive for the deposit and dissemination of scientific research documents, whether they are published or not. The documents may come from teaching and research institutions in France or abroad, or from public or private research centers.

L'archive ouverte pluridisciplinaire **HAL**, est destinée au dépôt et à la diffusion de documents scientifiques de niveau recherche, publiés ou non, émanant des établissements d'enseignement et de recherche français ou étrangers, des laboratoires publics ou privés.



Distributed under a Creative Commons Attribution - NonCommercial 4.0 International License

# Robustness of District Heating versus Electricity-Driven Energy System at District Level: a Multi-Objective Optimization Study

Jaume Fitó<sup>a,\*</sup>, Mathieu Vallée<sup>a</sup>, Alain Ruby<sup>a</sup>, Etienne Cuisinier<sup>a</sup>

<sup>a</sup> Univ. Grenoble Alpes, CEA, LITEN, DTCH, LSET, F-38000 Grenoble, France

## Abstract:

This article compares the robustness of the optimal choice of technologies for two Smart Energy Systems architectures at district level, illustrated by a case study representative of a newly built district in Grenoble, France. The electricity-driven architecture relies on the national electric grid, decentralized photovoltaic panels and decentralized heat pumps for heat production building by building. The alternative architecture consists of a district heating network with multiple sources and equipment for centralized production of heat. Those are a gas boiler plant, a biomass-driven cogeneration plant, a solar thermal collector field, and a geothermal heat pumping plant (grid-driven or photovoltaics-driven). Electric and heat storages are considered in both architectures. The sizing and operation of both architectures are optimized via linear programming, through a multi-objective approach (total project cost versus carbon dioxide emissions). Both architectures are compared at nominal scenario and at sensitivity scenarios. It is concluded that the electricity-driven architecture is less robust, especially to uncertainties in space heating demands (+150%/-30% impact on costs) and in heat pump performance (+35%/-15% in costs). Meanwhile, the multi-source architecture is less sensitive to space heating demands (+110%/-30%) and has negligible sensitivity to the rest of parameters except photovoltaic panels efficiency (+14%/-7%).

**Keywords:** District heating, Multi-energy networks, Multi-objective optimization, Model predictive control, Sensitivity analysis, Energy storage.

## Highlights:

- Decentralized electricity-driven architecture versus centralized district heating.
- Interconnected electrical, thermal and gas networks through various units.
- Optimal sizing by linear programming simulation and model predictive control.
- Sensitivity analysis of both architectures on performance parameters.
- Discrepancies observed between sensitivity of both architectures.

## Abbreviations:

CAPEX: Capital expenditures

CHP: Combined heat and power

CO<sub>2</sub>: Carbon dioxide

COP: Coefficient Of Performance

CREST: Centre for Renewable Energy Systems Technology

DH: District Heating

DHW: Domestic hot water

LHV: Lower heating value

LP: Linear Programming

MILP: Mixed Integer Linear Programming

OPEX: Operating expenses

PV: Photovoltaic

RT2012: French regulations on thermal performance of buildings

SH: Space Heating

SOC: State of charge (of storage units)

ST: Solar Thermal

TUS: Time use survey

# 1. INTRODUCTION

In France and in other countries, a large share of energy consumption is dedicated to satisfying the thermal demand of residential buildings [1]. While this demand has long been covered with fossil-fuels, it has to be quickly reduced in order to face challenges related to climate change, as well as for energy independence. Massive electrification, i.e., substituting fossil fuels with power-to-heat technologies, is one possible option for performing this shift, especially when considering renewable electricity sources.

Still, this transition process must take into account three major constraints. First, increasing the overall residential electricity consumption is not desirable. Indeed, a prospective study in France [2] recommends a slight decrease by 2050, while at the same time increasing the dependence of the residential sector on electricity. Second, the temporal mismatch between renewable electricity production and consumption for residential purpose (especially at yearly scale) must be accounted for [3]. Third, thermal renovation of the existing building stock will take time and may not be in phase with electrification and an increase of renewable production capacity. As a consequence, more realistic scenarios require not only electrification but also increased sector coupling, in particular between the electric and thermal networks, which can provide flexibility at different time scales (from instant to year) [4]. The interconnection of energy vectors leads to multi-energy systems, understood as multi-service and multi-fuel systems, and can outperform mono-energy systems both in techno-economic and environmental terms [5]. Within these systems, the diversity of actors as well as the intrinsic intermittence of renewables requires advanced strategies for energy management, leading to the concept of smart energy system [6].

## 1.1. Benefits of a multi-energy approach at district level

At the district level, multi-energy approaches are very relevant in combination with district heating. The interconnection of different energy networks can bring advantages both for the networks and the systems interconnecting them. This is illustrated, for instance, by Arabkoohsar et al [7], who proposed photovoltaic-thermal-cooling with heat and cold storages, capable of interacting with electric, heating and cooling networks. Such system outperformed the reference system (photovoltaic panels with batteries and a heat pump), mainly thanks to the multi-vector connections. In Finland, Paiho and Reda [8] pointed out trigeneration (production of electricity, heating and cooling) as a key enabling technology for future district heating systems. Su et al [9] also identified geothermal heat or power plants, waste-to-energy, and biomass-based power plants as key technologies to reach Finland's objective of carbon neutrality by 2035. Solar heat is also relevant for decarbonization purposes, although its insertion is more complex than just increasing the solar share, as pointed out by Mäki et al [10]. For cases like the Aalborg Municipality (Denmark), the evolution to 4th generation district heating (4GDH) was estimated to reduce total costs and primary energy consumption by 2.7% and 4.5% respectively. Other notable effects would be a roughly 30% improvement in heat pumps performance and at least a 2-fold increase in the uptake of excess heat from industrial processes [11]. Denmark faces a growing need for integrating non-combustion heat generation methods in district heating [12], and multi-energy approaches could be an answer to such need. In Sweden, diversification of sources and the subsequent evolution of district heating enabled an almost fossil-free energy mix years ago [13]. Current Swedish efforts are encouraged towards valorization of low-temperature recovered or recycled heat [14], among other efficiency aspects, where multi-energy architectures could be an enabler. Recently in Estonia, the Estonian Power and Heat Association (EHPA) has consolidated a methodology to assess district heating systems and acknowledge high efficiencies, as well as high shares of renewable energy. A quality Label is awarded to systems where at least 75% of heat is cogenerated, or at least 50% comes from renewables, or waste heat, or a combination of the three approaches [15]. In Lithuania,

diversification of district heating is encouraged in order to reduce the strong dependence on biofuels on which the country rests currently [16]. In Italy, Aste et al [17] suggested a wood biomass boiler coupled with combined heat and power (CHP), and combined with groundwater heat pumps coupled with photovoltaic systems. This low-carbon multi-energy system would cover all the thermal needs of a district in the Milan urban area, and a large portion of electricity needs. Electricity purchased from the national grid would range between 13.5% and 32% depending on the season, but electricity sold to the grid would range between 16.5% and 37%, therefore the district would be nearly zero-energy.

## **1.2. Optimal design of multi-energy networks**

Based on these encouraging results, many studies have been published concerning the co-planning [18] and co-optimization [19] of multi-energy networks. For example, Xie et al [20] proposed a new method for optimizing the operation of a multi-energy network comprising power, heat, cooling and gas loads, with multiple sources such as gas, wind or solar, and multiple conversion systems. Naughton et al [21] proposed an optimization approach for operating a multi-energy virtual power plant under uncertainty, showing that it could enhance the plant's flexibility and maximize market revenues. Several works investigate a wide range of possible options, not only concerning the available production and storage technologies, but also considering various ways of interconnecting networks. On a case study in Switzerland, Marquant et al. [22] indicate that an optimal design of district heating networks can reduce cost by 14.4% compared to a reference solution that does not consider any network possibility. Mavromatidis and Petkov [23] compare retrofitting options with multi-energy systems, and show that "retrofitting leads to lower emission levels, but significantly higher costs" while "interconnections improve both the economic and the environmental system performance". Jing et al. [24] compare a centralized and a decentralized solutions for a district in Shanghai, and show little difference in the obtained cost, when taking into account demand uncertainty.

## **1.3. Sensitivity of optimal design results**

As concluded by Gabrielli et al [25], the optimal design of a multi-energy network is a complex problem that requires investigating different objective functions. Their underlined total annual costs and carbon dioxide (CO<sub>2</sub>) emissions as two relevant objective functions. Besides, they pointed out the importance of describing well the dynamics between energy generation, conversion and consumption.

Si et al [26] presented a novel robust optimization problem in order to investigate the operational economy and reliability of an urban integrated multi-energy system. Among other interesting results, they found out that diversified solutions tend to be more robust and reliable in front of imbalances between energy supply and demand. Those solutions also proved to be more resilient to uncertainties, thanks to multi-energy conversion under their control algorithm.

The diversity of vectors makes the optimization more promising, but at the same time more complex. Energy and power analyses do not suffice, and it is necessary to resort to dynamic studies. Given the complex architecture, model predictive control is most recommendable for spotting efficient management. Coccia et al [27] demonstrated this by reducing backup electricity consumption by -71% in a residential multi-energy network including a district cooling system, photovoltaic panels and air-to-water heat pumps as backup.

Dahl et al [28] studied the sensitivity of an urban district heating system to cost variations. The system was coupled to an electricity system with penetration of wind technology. The thermal vector considered heat only boilers, combined heat and power (CHP) units, power-to-heat technologies and heat storages. The authors concluded that the optimal choice of

technologies was highly stable under cost variations, but the optimal capacities of CHP units and heat pumps were very uncertain if fossil fuels were allowed. In their perspectives, they recommend that future studies include solar heating, as they may alter dynamics significantly due to seasonality.

You and Kim [29] carried out a global sensitivity analysis on a smart energy network driven 100% by renewable energy sources. The sensitivity analysis was built on an optimization approach, with total annual costs as objective function. It also considered two scenarios, namely an electrified or hydrogen city.

The current state of the art is rich in assessments of either multi-energy networks or decentralized, renewables-driven solutions. It also contains several studies on the sensitivity of urban modeling to data available on buildings ages [30], or the benefits of thermal storage at multiple scales in district heating [31]. The search for robust optimization of hybrid systems that would be suitable in multi-energy networks has been also investigated [32].

#### **1.4. This paper**

The authors of this article think that there exists a research gap in evaluating and comparing the robustness of the technological choices in multi-energy district heating, in front of uncertainties on performance parameters. This article compares the sensitivity of two different systems architectures for district heating to several parameters. One architecture consists of heat production driven only by power, either from the network or from photovoltaic (PV) panels, with decentralized heat pumps. The other architecture considers district heating through a multi-source network including, electricity, gas and biomass, with centralized units for heat production. The comparison is based on technical-economic/environmental multi-objective optimization using model predictive control and considering both electric and thermal storages. The study addresses the research questions below:

- Which architecture performs better: electricity-driven or multi-source district heating?
- What is the optimal choice of technologies for each architecture?
- Do CO<sub>2</sub> emissions constraints change the optimal choice of technologies for each architecture?
- Which parameters are the most impactful on the project total costs?
- Which parameters are the most impactful on the optimal choice of technologies?

The remainder of this article is structured as follows. Section 2 presents the system modelled, the hypotheses, input data, optimization procedure, and configurations considered. Section 3 presents and discusses the main results, with a special focus on which configurations perform best and why the co-simulation approach with model predictive control was relevant. Lastly, Section 4 presents the main conclusions from this study and the authors' perspectives within the project that motivated this work.

## **2. MATERIALS AND METHOD**

The study consists in the multi-objective optimization (costs versus carbon emissions) of both the sizing and the operation of two different system architectures for district heating. The robustness of the optimal configuration is tested against variations in key parameters, and then compared between architectures. This section is structured in four parts. The first part describes the district under study, and the two architectures under evaluation for the heating network that covers its demands. The second part introduces and discusses the main hypotheses and input parameters. The third part presents and justifies the demand profiles used for residential electricity, space heating and domestic hot water (DHW) production. The choice of profile generator is briefly discussed, too. The fourth and final part presents

relevant aspects about the modeling of the study case, plus the parameters (and value ranges) considered for sensitivity analysis.

## 2.1. Case description

The Cambridge case study (Fig. 1) is inspired on a real district in the city of Grenoble (France). This study case is an updated version of the one used in previous research works [33], [34]. The Government of this district has an ambitious target of energy performance. Namely, around 30% lesser consumption of fuel with respect to the French RT2012 standard. This district benefits from two interesting thermal opportunities. One of them is a nearby phreatic table that can be exploited as geothermal source. The other one is a nearby river, the Isère, which can enable free cooling as a resource. This district and its buildings have been the target for numerous studies on energy efficiency and ecological transition. Those studies have yielded databases with abundant information on consumption and operation. Later, a series of research projects have refined those data and made them robust for other studies.

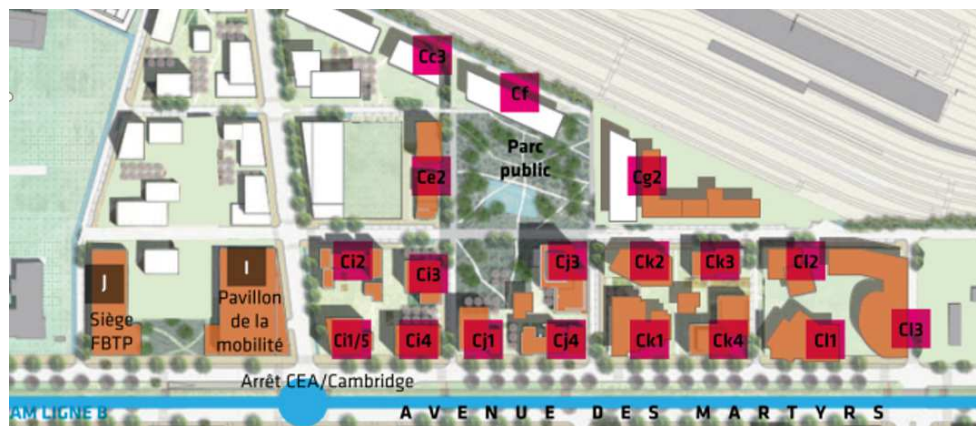
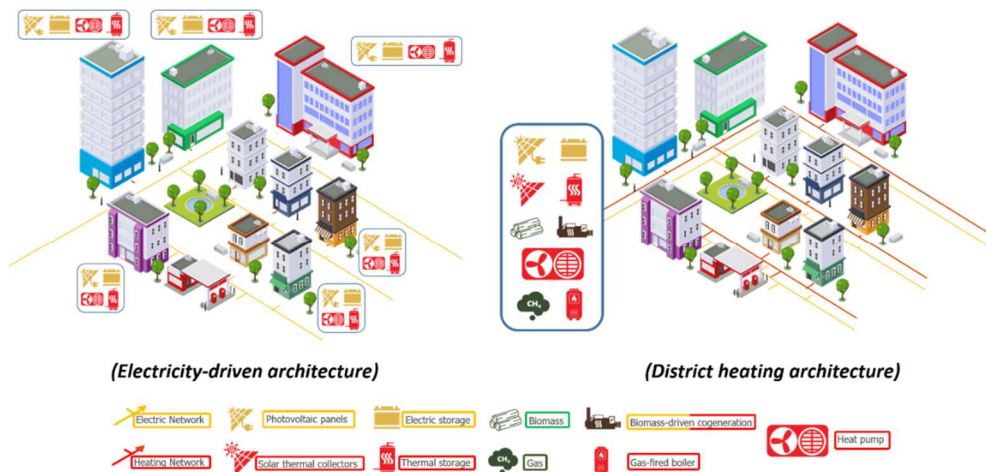


Figure 1. Schematic representation of the “Cambridge” district (and its buildings) in the city of Grenoble, France.

The study comprises 13 residential buildings, totaling 500 dwellings approximately. The reference architecture (Fig. 2, left) of the system for residential heating considers decentralized heat pumps, connected to the electric grid. An alternative architecture (Fig. 2, right) is currently under study in the framework of the DISTRISIM project. It would consist of a combination of an electrical and a thermal network, with centralized heat production systems and a gas-driven supply system. The study envisages also the decentralized production of electricity by the mean of PV panels on the rooftop of each building. The complexity of the case study consists in coupling the prospective thermal network with the existing electrical network. While interconnections between networks may take place at different scales (from one building to an entire continent), the district scale presents numerous advantages.



**Figure 2.** Schematic representations of the two architectures evaluated in this study.

Firstly, a diversity of technologies and applications, which enables decentralization of the electric grid by integration of renewable production systems with approaches for energy flexibility. Secondly, a sufficient level of spatial resolution, allowing to study the underlying phenomena. Thirdly, the availability of measured data, which enables validation of the results. Lastly, the possibility of upscaling the results, to the framework of a city, territory or a region. Of course, such scaling requires adaptation of the algorithms and processor capacities, but the general methodology remains the same.

Thus, the case study here described is relatively realistic, because most of the data come from a real district that represents a modern eco-district with mixed sources. The necessary information for optimizing the sizing is available: location of the production and storage units, limitations of the network such as maximal power, temperature levels and needs for expansion... At the same time, this case study gives some margin for research studies, since variations in the hypotheses are possible.

## 2.2. Hypotheses and input data

This study rests on the major hypotheses below:

- The entire interconnected system is under the control of one operator, who can manage it as convenient for addressing the whole district's needs. Contexts where different operators manage the units would introduce intermediate constraints that fall out of the scope of this article.
- The calculations do not consider limits to the space available for the implementation of storage units (thus, unlimited storage capacity) and solar generation units. However, we consider possible limits in the discussion of results.
- Pipes diameters and cable sections are fixed (i.e. they are not optimization variables).
- The geospatial implementation of the network is not an optimization objective, since it is rather a topological issue than an energetic issue.
- The environmental analysis does not account for embodied energy and CO<sub>2</sub> emissions are considered only at operation time (no life-cycle analysis).
- Startup and shutdown times are neglected for all units [35].

Table 1 presents input data for the model used in this study. For storage units, the efficiency shown in the table applies to both the charge and discharge processes. Self-discharge of storage units is expressed as a daily percentage of energy stored. Unless otherwise stated, minimal output power of all units is 0 kW.

The effect of scale on certain parameters was accounted for. For example, photovoltaic panels are generally more expensive at smaller scales. Since the electricity-driven decentralized solution considers installing panels by buildings, and the multi-source

centralized solution does so for the whole district, their capital expenditures (*CAPEX*) were adjusted. Thus, the *CAPEX* of photovoltaic panels is higher for the electricity-driven architecture (1050 €/kW<sub>p</sub>) than for the multi-source architecture (750 €/kW<sub>p</sub>). The same effect can be noticed on the *CAPEX* of heat storage: 40 €/kWh in the electricity-driven architecture versus 30 €/kWh in the multi-source architecture. The same applies for the *CAPEX* of the heat pump (1200 €/kW versus 1000 €/kW) and its operating expenses (*OPEX*) (6.0 %<sub>CAPEX</sub> versus 3.5 %<sub>CAPEX</sub>).

Non-pressurized thermocline water tanks were assumed as thermal storage units. For these kinds of units, Mouret et al report heat losses of 0.5 %/day for temperature differences up to 45 °C between the hot and cold water contained within the tank (page 161 of [36]). The value of 0.5 %/day applies to fully charged storages of capacities ranging from 100 m<sup>3</sup> to 12000 m<sup>3</sup>. Losses increase at smaller scale, therefore a value of 3.0 %/day was set in the electricity-driven architecture based on extrapolations from the correlations in [36] and [37]. Based on literature, full charging/discharging times of thermocline units can be as low as 3 hours. Consequently, the maximal charge/discharge powers for these units was supposed 33% of their maximal capacity.

**Table 1.** Input parameters and values. Case A and Case B refer to electricity-driven and multi-source architecture, respectively.

Unit	Parameter	Value (Case A)	Value (Case B)	Units	Source(s)
Economics, overall	Observation period	20	20	y	[38]
	Discount rate	7	7	%	[38]
	Electricity price	0.16	0.16	€/kWh	[39]
Solar PV field	CAPEX	1050	750	€/kW <sub>p</sub>	[40]
	OPEX	5	2	% <sub>CAPEX</sub>	[40]
PV converter	Efficiency	95	95	%	[40]
Electric batteries	Efficiency	90	90	%	[40]
	Self-discharge	0.01	0.01	%/day	[40]
Electric network	Initial SOC	50	50	%	Hypothesis
	Final SOC	50	50	%	Hypothesis
	Max. charge	33	33	% <sub>CAPACITY</sub>	[31], [36]
	Max. discharge	33	33	% <sub>CAPACITY</sub>	[31], [36]
	CAPEX	220	220	€/kWh	[40]
	OPEX	2	2	% <sub>CAPEX</sub>	[40]
Thermal network	Efficiency	100	100	%	Hypothesis
Solar thermal collector field	Efficiency	N/A	95	%	[41]
	CAPEX	N/A	500	€/kW <sub>th</sub>	[41]
Thermal storage unit	OPEX	N/A	7.5	% <sub>CAPEX</sub>	[41]
	CAPEX	N/A	200	€/m <sup>2</sup>	[40]
Thermal storage unit	OPEX	N/A	1.0	% <sub>CAPEX</sub>	[40]
	Max. charge	33	33	% <sub>CAPACITY</sub>	[31], [36]
Thermal storage unit	Max. discharge	33	33	% <sub>CAPACITY</sub>	[31], [36]
	Charge/discharge eff.	100	100	%	[31], [36]
Thermal storage unit	Self-discharge	3.0	0.5	% <sub>STORED/day</sub>	[31], [36], [37]
	Initial SOC	50	50	% <sub>CAPACITY</sub>	-
Thermal storage unit	Final SOC	50	50	% <sub>CAPACITY</sub>	-
	CAPEX	40	30	€/kW <sub>th</sub>	[42]
Heat pump	OPEX	2	2	% <sub>CAPEX</sub>	[40]
	COP	3	3	kWh <sub>th</sub> /kW <sub>el</sub>	-
Heat pump	Inlet temperature	10	20	°C	-
	Outlet temperature	65	80	°C	-
Heat pump	CAPEX	1200	1000	€/kW	[40]
	OPEX	6.0	3.5	% <sub>CAPEX</sub>	[40]
Gas boiler plant	Efficiency	N/A	90	%	[40]
	CAPEX	N/A	500	€/kW	[40]
Gas boiler plant	OPEX	N/A	4	% <sub>CAPEX</sub>	[40]
	Cost of gas	N/A	0.55	€/kg CH <sub>4</sub>	[43]
Gas boiler plant	LHV of gas	N/A	13.83	kWh/kg CH <sub>4</sub>	[44]
	CO <sub>2</sub> content of gas	N/A	3.36	kg CO <sub>2</sub> /kg CH <sub>4</sub>	[44]
Biomass-driven cogen. plant	Efficiency (thermal)	N/A	60	%	[40]
	Efficiency (electrical)	N/A	30	%	[40]
Biomass-driven cogen. plant	Density of biomass	N/A	700	kg/m <sup>3</sup>	Handbook
	Max. biomass uptake	N/A	100	kg/h	Hypothesis
Biomass-driven cogen. plant	LHV of biomass	N/A	4.00	kWh/kg	Handbook
	Buying price of biomass	N/A	0.12	€/kg	[45]
Biomass-driven cogen. plant	CAPEX	N/A	800	€/kW	[40]
	OPEX	N/A	4	% <sub>CAPEX</sub>	[40]

The biomass cogeneration unit was modelled as a non-pilotable unit that produces heat and electricity at the same time, with efficiencies of 60% and 30% respectively. The *CAPEX* of this unit refers to total production (i.e. heat plus electricity). For a minimally realistic



simulation of this unit, a constraint was applied on the maximal uptake of biomass, as this resource is quite more limited than solar irradiation or ground source heat. A constraint of 100 kg/h was selected. This constraint can make results interesting for countries whose district heating systems depend heavily on biomass. Those countries could interpret the results as a projection of how their energy mix could look like after reducing dependence on biomass.

Biomass is generally considered as low-carbon in France. Indeed, reports from the ADEME, i.e. the French Agency for Ecological Transition [46] assume 0 CO<sub>2</sub> emissions for wood-burning biomass in DHC. This is based not only on the fact that a tree, throughout its lifetime, captures and neutralizes as much CO<sub>2</sub> as its biomass releases upon combustion, but also considering that most regions in France have local biomass availability which reduces side emissions due to transport. In particular, this case study is located in a French region (Auvergne-Rhone-Alpes) that is highly populated with trees overall.

The hypothesis would be different in other countries. For instance, the Danish Energy Agency suggests 24-30 gCO<sub>2</sub>/kWh of energy produced via biomass-driven cogeneration [40]. Also, competition with other potential use of biomass (agriculture, soil protection) should be taken into account, but this would have to be done in a complete Lifecycle Analysis which goes beyond the scope of this paper.

### 2.3. Demand profiles

The only empirical data available for this study were monthly consumptions of energy for each of the 13 buildings. Since the optimizations required yearly profiles at an hourly time step, synthetic profiles had to be constructed. The CREST demand tool, created by the Centre for Renewable Energy Systems Technology (UK), was selected for such purpose [47]. Amongst the available open-source profile generators, the CREST tool provided, for this study, the best trade-off between model accuracy and calculation speed. Although the tool has been validated for the English and Indian residential sectors, and not the French one, the validation procedure is quite rigorous and based on an extensive list of indicators and data sets [48], [49].

The tool allows simulating yearly demand profiles of specific electricity, space heating and domestic hot water production for one dwelling. It allows selecting the number of occupants, ranging from one to six. The tool contains its own database of domestic appliances, with their energy consumptions. Occupants' behaviors are simulated stochastically, by the mean of first-order Markov chains at a 10 minute time step, generated from the UK 2005 Residential Time Use Survey (TUS) [50].

Simulations were launched for the total number of dwellings in the 13 buildings (ca. 500 dwellings), with a random number of occupants at each dwelling. The individual profiles were aggregated on a building basis for simulating the electricity-driven architecture. Then, they were aggregated for the district in order to simulate the district heating architecture. The resulting profiles are shown in Fig. 3. The yearly profiles are shown, with 24-h samples next to them.

The profile of electric needs consists of a baseline for the whole year (Fig. 3a) with oscillations between 50 kW and almost 600 kW. This profile does not seem affected by seasonality. On a daily basis, it shows a peak in the evening that is quite consistent with the residential sector. However, it does not show a peak in the morning, which one could expect from residential buildings.

The profile of space heating needs shows clear seasonality, as in the vast majority of needs take place in winter. However, the demand drop of late spring and its rise of early autumn are rather stiff. This may be a shortcoming in the modelling. Despite that, the profile was

considered acceptable since buildings in the Cambridge district are rather new and well-isolated.

The demand profile for domestic hot water production consists of a baseline, like the electric profile. However, it shows some seasonality, because demands increase slightly in winter. Still, peak instantaneous needs revolve around 300 kW for the whole year. On a daily basis, the tool represents well the typical peaks in the morning and evening. Nevertheless, consumption between 11pm and 4am is typically zero, which might be unrealistic. In France, boilers are sometimes programmed for slowly heating water at night, aiming at having the full reservoir ready by 6am.

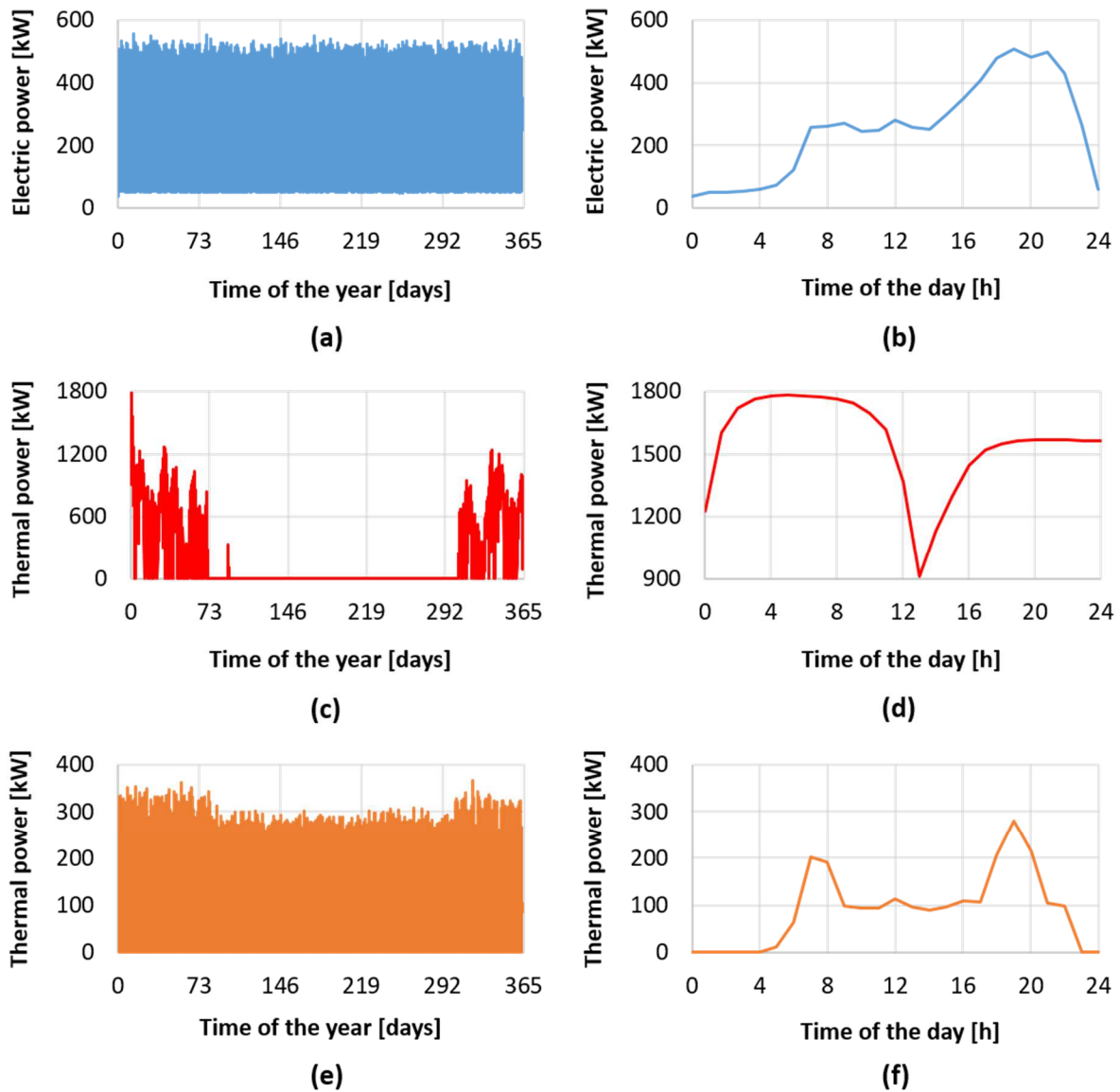


**Figure 3.** Yearly profiles and daily samples of electricity (a and b), heating (c and d) and domestic hot water (e and f) needs.

## 2.4. Network architectures and sensitivity scenarios

The study was approached through operational optimization. This method consists in modelling dynamically both the system and its control system, by the mean of linear

mathematical constraints. This is nowadays the reference method, as noted by Cuisinier et al [51]. Figure 4 displays the architectures for the prospective system, as implemented in the homemade PERSEE tool [52]. This tool translates the system into a linear programming (LP) problem, based on well-known equations in LP (see an example in [52], or in [53] for MILP, i.e. Mixed-Integer Linear Programming).

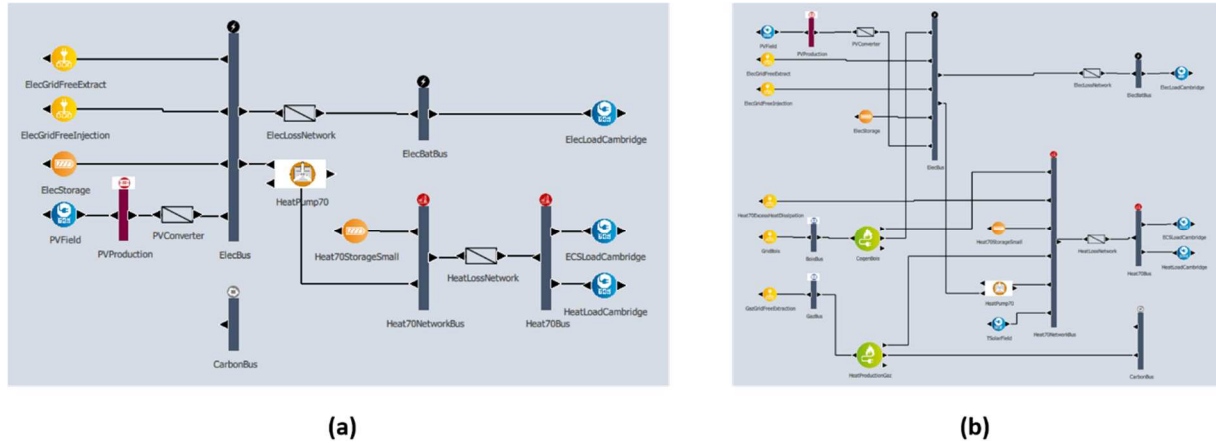


**Figure 4.** Modeling of the prospective system, with both architectures, on the PERSEE tool.

The optimization code works with the following energy-related vectors:

- **Electricity.** This vector concerns the following units in the system: the French national electric network, the electric needs of the buildings within the district, the electric output of the biomass-driven cogeneration plant, the electric input of the heat pumps, and the electric batteries.
- **Heat.** The supply temperature of the district heating network is assumed as 80 °C. In the architectures considered for this study, the need for heat at that temperature is coverable by the gas boiler plant, or the biomass-driven cogeneration plant, or the solar thermal panels, or the heat pumps in certain architectures. The return temperature is 40 °C. In the electricity-driven architecture, as heat pumps are decentralized, their heat production is supposed to be a 65 °C.
- **Gas.** This vector concerns the input of the gas boiler plant, and the gas network that ensures that input.
- **Biomass.** This vector concerns the input of the biomass-driven cogeneration plant.
- **CO<sub>2</sub> emissions.** This vector, rather than serving any particular balance within the model, is an informative vector in order to account for total emissions.

The optimizations consider the costs of excess heat dissipation from the solar thermal collectors. Those costs are determined through the correlation below:

$$c_{ST-diss} = Q_{excess}^{ST\ coll} [kW_{th}] \cdot 0.0275 \left[ \frac{kW_{el}}{kW_{th}} \right] \cdot c_{el}^{network} \left[ \frac{\text{€}}{kW_{el}} \right] \quad (1)$$

With  $Q_{excess}^{ST\ coll}$  the excess heat generated by solar thermal panels,  $c_{el}^{network}$  being the cost of network electricity (a flat 0.16 €/kW<sub>el</sub> in most scenarios), and the 0.0275 a correlation factor between heat dissipated and electricity consumed for such dissipation (operation of aerothermal equipment). This correlation comes from engineering experience from the authors' laboratory [54].

The following parametric studies were conducted in order to verify robustness of the technical solutions to uncertainties in the parameters below:

- Ratio of space heating demands.
- Coefficient Of Performance (*COP*) of the heat pump.
- Performance of photovoltaic panels.
- Performance of solar thermal collectors.
- Heat losses of the thermal storage unit.
- Variability in price and CO<sub>2</sub> emissions of grid electricity (versus constant values).
- Taxes on CO<sub>2</sub> emissions.

Table 2 shows the range of values considered for each parameter. The study focuses on parameters that exist in both architectures, for the sake of comparison.

**Table 2.** Values of the constraints applied throughout the sensitivity analysis.

Parameter	Lower bound	Nominal value	Upper bound	Units
Space heating demands	-50%	See section 2.3	+200%	GWh/y
COP of the heat pump	2 (-33%)	3	4 (+33%)	-
PV panels efficiency	10	15	20	%
ST collectors efficiency	60	70	80	%
Charge/discharge eff. of batteries	0.85	0.9	0.95	%
Heat storage losses (architecture A)	0.5	3.0	5.0	%/day
Heat storage losses (architecture B)	-	0.5	5.0	%/day
Grid electricity price	Variable	0.16 (Fixed)	Variable	€/kWh <sub>el</sub>
Grid electricity emissions	Variable	0.057 (Fixed)	Variable	kgCO <sub>2</sub> /kWh <sub>el</sub>
Tax on CO <sub>2</sub> emissions	-	100	250 (+150%)	€/tCO <sub>2</sub>

Space heating is heavily dependent on building design, localization and thermal insulation. In France, the average load for space heating is around 150 kWh/m<sup>2</sup>/y [55] but in new buildings, it needs be as low as 50 kWh/m<sup>2</sup>/y due to the current RT2012 regulation. Thus, it is interesting to check the effects of different heating loads.

Variations considered for the Coefficient Of Performance (*COP*) of the heat pump correspond to the expectable temperature lifts in both architectures. Causes for such lifts are different in each architecture. In the electricity-driven one, the output temperature requirement is constant but the inlet temperature may vary, as aerothermal heat pumps are supposed. In the District Heating architecture, the input temperature is constant thanks to a geothermal source (see subsection 2.1), but the output temperature requirements may fluctuate due to inertia in the district network.

Efficiency ranges for photovoltaic panels, solar thermal collectors and electric batteries are plausible given the current state of the art for such technologies. The same applies to heat storage losses. Concerning the specific price and CO<sub>2</sub> emissions of grid electricity, two scenarios were considered. The first one consists of a fixed price and fixed emissions throughout the year (see column “Nominal value”). The second one consists of hourly profiles of price and carbon emissions, whose yearly averages are the same as the fixed values used in the nominal scenario. As for carbon taxes, the nominal value corresponds approximately to the current scenario in France, while the upper bound is the value that some organizations advise in order to favor ecological transition.

The reference electricity price used in the simulations is based on the data available from the ENTSO-E Transparence platform [56]. This data has been adjusted with a constant bias in order to take into account transportation and distribution costs as well as the non-residential final consumer subscription. This constant bias is calculated in function of the average 2013-2018 values for France, retrieved from the Eurostat database [57]. The electricity price’s yearly average value is 0.0758 €/kWh.

### 3. RESULTS AND DISCUSSION

This section is structured in three parts. The first part displays and discusses the costs-emissions Pareto front for both architectures, and the essential differences between the two. The second part analyzes and compares the sensitivity of both Pareto fronts to the parameters discussed in Table 2. The third and last section focuses on the effects of different space heating demands, which turned out to have not only high consequences on total cost, but also on the optimal choice of technologies.

### 3.1. Comparison of architectures at nominal scenario

Figure 5 displays, for each architecture at the nominal scenario, the project's total cost as a function of the carbon emissions constraint applied on the system. Total cost refers to net present costs, including the *CAPEX* and the *OPEX*. Carbon emission constraint refers to the maximum emissions of CO<sub>2</sub> allowed in one year. For the sake of analysis, total costs are also displayed by component, in the form of stacked bars. For the sake of comparison, axes on both graphs cover the same ranges and have the same increments, and a dashed line compares total costs at unconstrained scenarios.

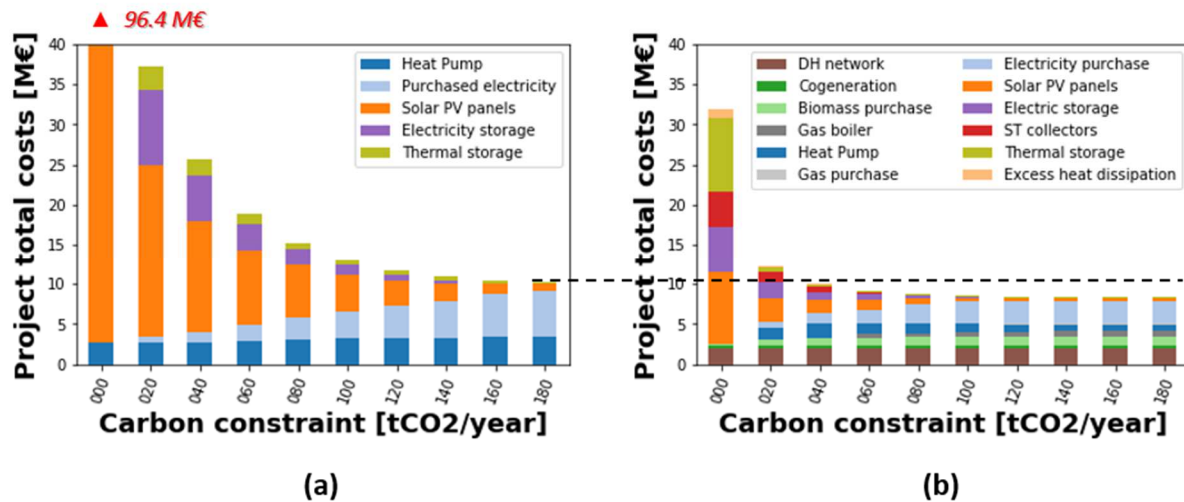


**Figure 5.** Costs vs Emissions Pareto front at nominal scenario. (a) Electricity-driven architecture; (b) District heating architecture.

In the electricity-driven architecture, the right-most value on the x-axis corresponds to an unconstrained scenario (total emissions are 173 tCO<sub>2</sub>/y versus the constraint of 180 tCO<sub>2</sub>/y). For the multi-source district heating (DH) architecture, an unconstrained scenario would require carbon emissions limitations of 331 tCO<sub>2</sub>/y or higher (due to the possibility of using a cost-efficient gas boiler). The right-most scenario on the graph is thus constrained. Yet, total costs barely change from 180 tCO<sub>2</sub>/y to 331 tCO<sub>2</sub>/y, and the choice of technologies does not change at all (just their sizes do).

Both graphs display the well-known tendency wherein costs increase as the limitation on CO<sub>2</sub> emissions becomes heavier, resulting in a Pareto front. At carbon-unconstrained design, the electricity-driven architecture relies mostly on electricity from the grid and a heat pump. The optimizer suggests a small investment in solar PV panels as well, which should correspond to the size that optimizes the self-consumption and -production indices. In the multi-source DH architecture, the optimal solution is an energy mix, even at unconstrained design. The biomass cogeneration plant operates at its maximal capacity in most of the cases, under the imposed limitation of 100 kg/h of biomass (read description for Table 1).

As expected, heavier constraints on CO<sub>2</sub> emissions trigger the use of renewable sources, i.e. solar panels in this study. Accordingly, carbon-intensive resources such a gas (3.36

kgCO<sub>2</sub>/kgCH<sub>4</sub>, or 0.243 kgCO<sub>2</sub>/kWh<sub>th</sub>) or grid electricity (0.057 kgCO<sub>2</sub>/kWh<sub>el</sub> in the French context) are gradually left behind. However, in the district heating architecture, the irruption of renewables occurs only at more constraining CO<sub>2</sub> limitations than in the electricity-driven architecture. This is due partly to the presence of the biomass cogeneration plant, but mostly because of the demand pooling effects, which maximize the coverage of demands by solar panels.

Differences in the choice of technologies become more evident at constraints of 60 tCO<sub>2</sub>/y or lower. That is where the multi-source DH architecture starts resorting to solar thermal collectors. Let the readers recall that solar thermal collectors are not available in the electricity-driven architecture. The zero-emission scenario shows the most evident discrepancies. The DH architecture finds its optimum in a balance between the PV / batteries pairing and the ST / storage pairing. Meanwhile, the electricity-driven architecture relies heavily on PV panels and batteries, with a very small investment in thermal storage. The causes for this discrepancy are higher investment costs in thermal storage (40 €/kWh versus 30 €/kWh) and greater heat losses (3 %/day versus 0.5 %/day) of the thermal storage at smaller scales in comparison to larger scales.

The different sensitivities to carbon constraints are also noticeable. When going from unconstrained to zero-emission scenarios, total costs increase by 4-fold for the DH architecture, but by 9-fold for the electricity-driven architecture. Higher specific investment costs of equipment at smaller sizes are one reason for this discrepancy. The other reason is the fact that demand pooling allows shaving peak demands. While the DH architecture has centralized production units, the electricity-driven architecture has decentralized units, leading to higher overall investment.

Next subsection focuses on the sensitivity of each scenario to the parameters pointed out in Table 2.

### 3.2. Sensitivity to selected parameters

Sensitivity analysis was done by changing parameter values, one parameter at a time. Table 3 describes, for each scenario, the parameter that has been modified and its new value.

**Table 3. Description of the scenarios for sensitivity analysis.**

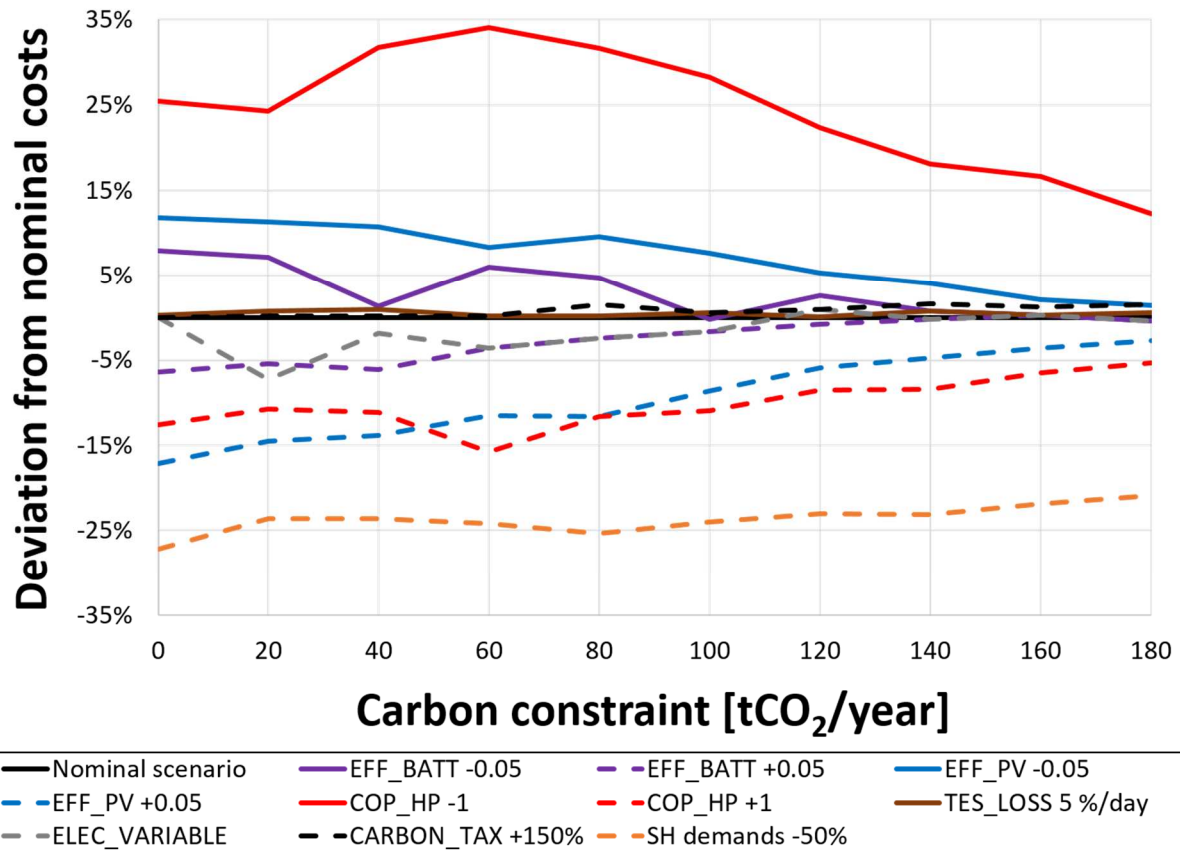
Scenario name	Parameter modified	Value (modified)	Units
Nominal scenario	None	-	-
EFF_ST -0.10	Efficiency of solar thermal collectors	0.60	kW <sub>th-out</sub> /kW <sub>th-in</sub>
EFF_ST +0.10		0.80	
EFF_BATT -0.05	Charge/discharge efficiencies of electric batteries	0.85	kW <sub>e</sub> /kW <sub>el</sub>
EFF_BATT +0.05		0.95	
EFF_PV -0.05	Efficiency of solar photovoltaic panels	0.10	kW <sub>el-out</sub> /kW <sub>th-in</sub>
EFF_PV +0.05		0.20	
COP_HP -1	Coefficient Of Performance of the heat pump	2	kW <sub>th-out</sub> /kW <sub>el-in</sub>
COP_HP +1		4	
TES_losses 5%/day	Daily energy losses of the thermal storage unit	5	%/day
ELEC_VARIABLE	Hourly profile of electricity price	Variable (yearly mean = 0.16)	€/kWh <sub>el</sub>
	Hourly profile of electricity CO <sub>2</sub> content	Variable (yearly mean = 0.057)	kgCO <sub>2</sub> /kWh <sub>el</sub>
CARBON_TAX +150%	Taxes on CO <sub>2</sub> emissions	250	€/tCO <sub>2</sub>
CAPEX_BIO +200%	CAPEX of biomass-driven cogeneration unit	2400	€/kW <sub>th-out</sub>
FUELCOST_GAS +200%	Cost of gas fuel	1.65	€/kgCH <sub>4</sub>

Figure 6 shows, for the electricity-driven decentralized architecture, relative sensitivity of total costs to selected parameters, for different carbon constraints. In other words, the graph displays the sensitivity of the Pareto front.

Space heating demands were the most impactful parameter in this study, only second to carbon constraints. Halved heating demands can reduce costs by 21% to 27%, depending

on the position within the Pareto front. Tripled heating demands can increase costs by 100% to 150% (not shown in this graph, see Fig. 9).

The *COP* of the heat pump was the second-most impactful parameter. A decrease in *COP* of 33% (i.e. from 3 to 2) increased costs by 12% to nearly 35%. Conversely, an increase in *COP* of the same magnitude cut costs back by 5% to 15%. Note that the effects of efficiencies on costs are inversely proportional.



**Figure 6.** Sensitivity of the electricity-driven architecture to selected parameters, at different carbon constraints. Refer to Table 3 for description of the scenarios in the legend.

It is also noteworthy that the profiles of costs increases/decreases vs carbon constraint are not symmetrical. The reason is that the amount of electricity required to run the heat pump evolves non-linearly with respect to the *COP*. A drop in *COP* of -33% causes +50% electricity required, while an increase of +33% only allows for -25% electricity required. In other words, a drop in *COP* is more penalizing than an increase in *COP* is rewarding. Thus, improving the *COP* can reduce costs notably, but this has its limits. The guideline should rather be to avoid a low *COP* than to aim for a very high *COP*. Besides, a very high *COP* might have its drawbacks if the input heat is limited and/or paid for. For instance, waste heat purchased from an industrial partner somewhere in the district.

Interestingly, peak sensitivity to this parameter does not occur at extreme points of the Pareto front. As explained in the previous paragraph, a drop in *COP* leads to an increase in electricity needs. The optimizer manages that increase differently, depending on the carbon constraint. In less constrained scenarios ( $\geq 120$  tCO<sub>2</sub>/y), it can just buy more electricity from the grid. As grid electricity is relatively not expensive, costs do not greatly increase. In very constrained scenarios ( $\leq 20$  tCO<sub>2</sub>/y), more solar panels need to be installed to compensate

for the lower *COP*, but the investment in panels is very high anyway. In intermediate scenarios, the increase in panels' size is most impactful with respect to total costs.

Figure 7 is a summary of the sensitivity of the DH architecture to the different parameters considered. It is displayed in the form of relative deviations with respect to total project costs at nominal scenario.

As expected, sensitivity increases at heavier carbon constraints, and some parameters are more influential than others are. Nevertheless, depending on the scenario and parameter considered, deviations may or may not be negligible.

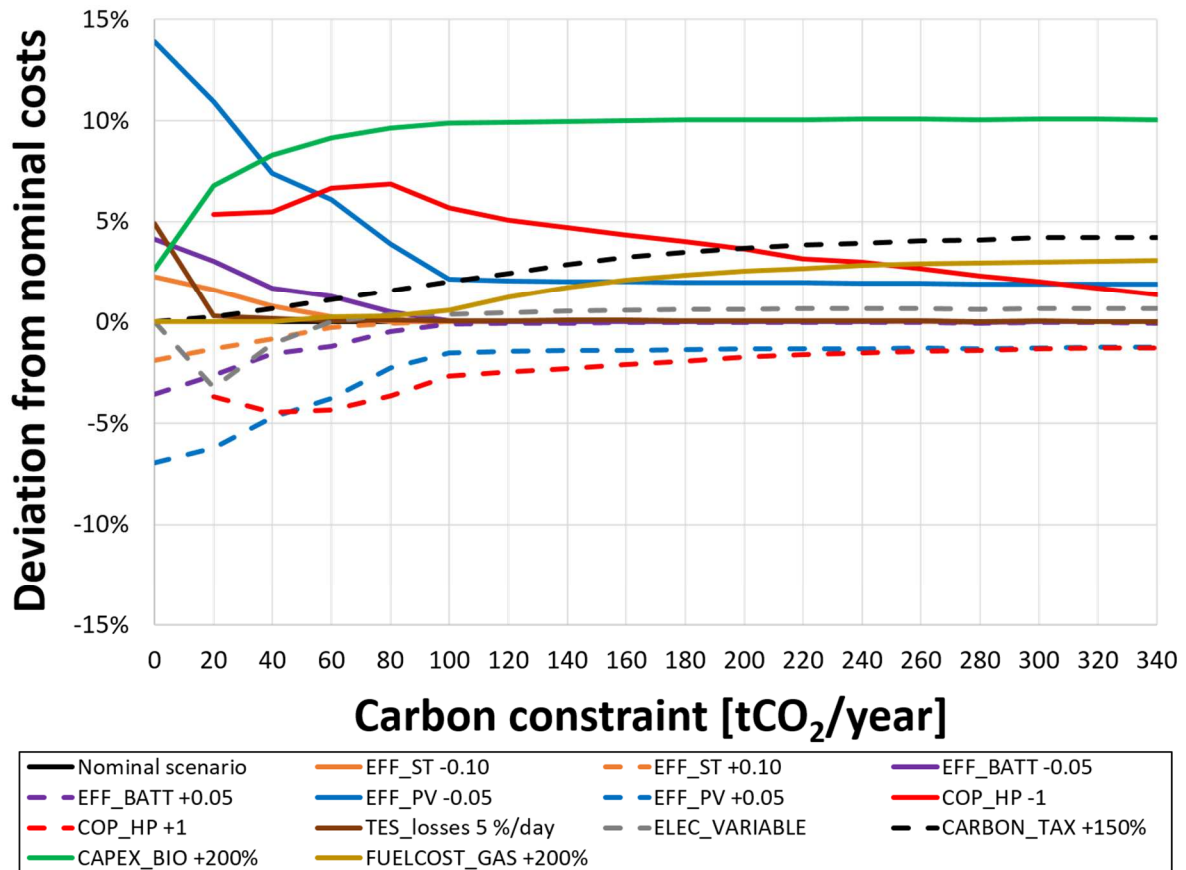


Figure 7. Sensitivity of project total costs at different carbon constraints, for the multi-source district heating architecture. Refer to Table 3 for description of the scenarios in the legend.

Variations of +/- 5% in the efficiency of PV panels only have noticeable effects at carbon constraints lower than 80 tCO<sub>2</sub>/y. This is understandable, as only constrained scenarios rely on solar panels. Yet, even in the most constrained scenarios, sensitivity to this parameter is almost negligible (5% or lesser deviations). This is a notable difference with respect to the electricity-driven architecture, where the effects of this same parameter were not negligible for most of the scenarios. As explained for the nominal case (see subsection 3.1), the cause is that the DH architecture enables demand pooling and therefore peak load shaving.

The effects of the heat pump *COP* are mostly negligible, too. Upper and lower values of 4 and 2 were considered (i.e. +/- 33%, respectively). Even though this margin is larger than that considered for the *CAPEX* of PV panels, the effects remain negligible. Note, however, that the profile of relative deviations differs from those of other parameters. It is linked to the usage of the heat pump. As seen in Fig. 5, the greatest investments on a heat pump (and thus its size) take place at constraints between 20 tCO<sub>2</sub>/y and 80 tCO<sub>2</sub>/y. Sensitivities are



accordingly higher. At the zero-emission scenario, there is no sensitivity because there is no heat pump.

Variations in the efficiency of ST collectors has negligible impact. Heat losses in the thermal storage have an impact only at very pessimistic scenarios. Here, up to 5 %/day and 10 %/day were considered, while the nominal case for large scales is rather 0.5 %/day. It is thus concluded that this parameter does not seem to have a great impact on total costs.

Results indicate that the CAPEX of the biomass-CHP unit has a light impact on total costs. Even with three times the nominal CAPEX, maximum increase on total cost is around 10%, and corresponds directly to multiplying the cost of the biomass-CHP unit by 3. The optimal choice of technologies remains unchanged, except in the unconstrained scenario, where the optimizer tends to reduce the size of biomass-CHP (-3%) and increase the size of a heat pump (+5%). Under 100 tCO<sub>2</sub>/year, the sensitivity seems lower, however this is only due to an overall increase in the total costs.

Despite tripled prices for the fuel gas, the impact on total costs or on the optimal choice of technologies was close to negligible. Even with nominal prices (left), the optimal solution includes only a small investment in gas. This investment decreases gradually as the carbon constraint becomes heavier, and the heat pump tends to substitute the gas boiler. If gas prices were to be tripled, the heat pump would further replace the gas boiler. Yet, gas would still not be completely phased out, except in heavily constrained emission scenarios (< 40 tCO<sub>2</sub>/year). This could probably mean that gas is the last resort used by the optimizer in order to tackle very specific demand peaks throughout the year.

### **3.3. Detailed effects of space heating demands**

In this section, we consider the sensitivity to different level of space heating (SH) consumption, corresponding to various level of building performance. The reference case in the previous section is based on a SH consumption of 50 kWh/m<sup>2</sup>/y, which corresponds to the required level of performance for new buildings under the current (RT2012) French regulation. As alternatives, we consider (1) a SH consumption of 150 kWh/m<sup>2</sup>/y, which is the average level of performance for apartment blocks in France, (2) a SH consumption of 25 kWh/m<sup>2</sup>/y, which is representative of very efficient buildings. Since the yearly energy consumption for SH, DHW and specific electricity are approximatively at the same level in the reference case, it means that the share of SH jumps to 60% or drops to 20% of the total energy consumption of the district, respectively.

Figure 8 presents and compares the sensitivity of the total cost with respect to the SH consumption level. As expected, increased or decreased space heating consumption results in an increase or decrease in total costs, respectively. The two architectures, however, seem to be similarly cost-sensitive to these variations (Fig. 9). The electricity-driven architecture is just slightly more sensitive to increases in heating demands.

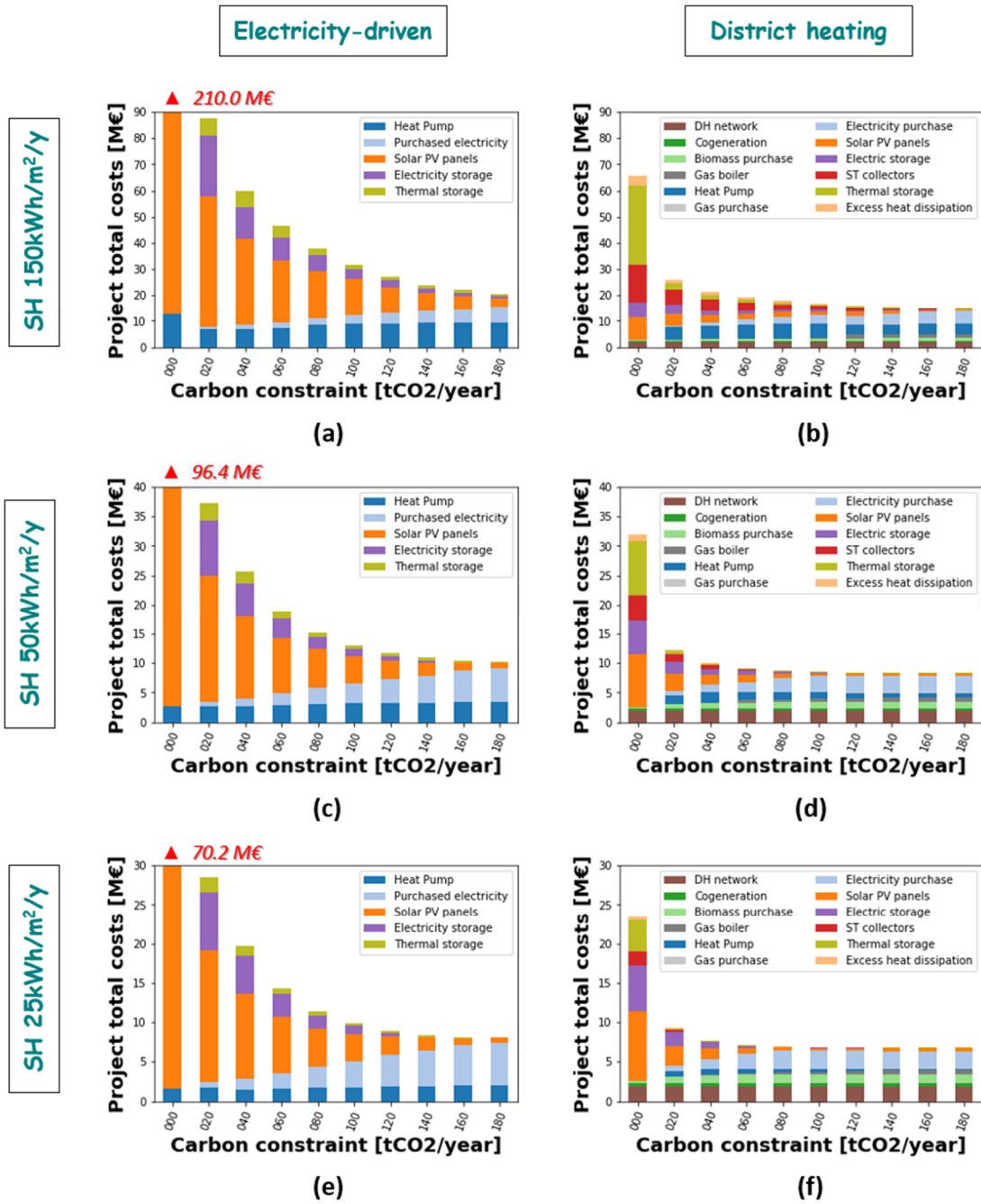


Figure 8. Robustness of the design to uncertainties in space heating demands. Electricity-driven architecture with tripled (a), nominal (c) and halved (e) heating demands versus district heating architecture with tripled (b), nominal (d) and halved (f) heating demands.

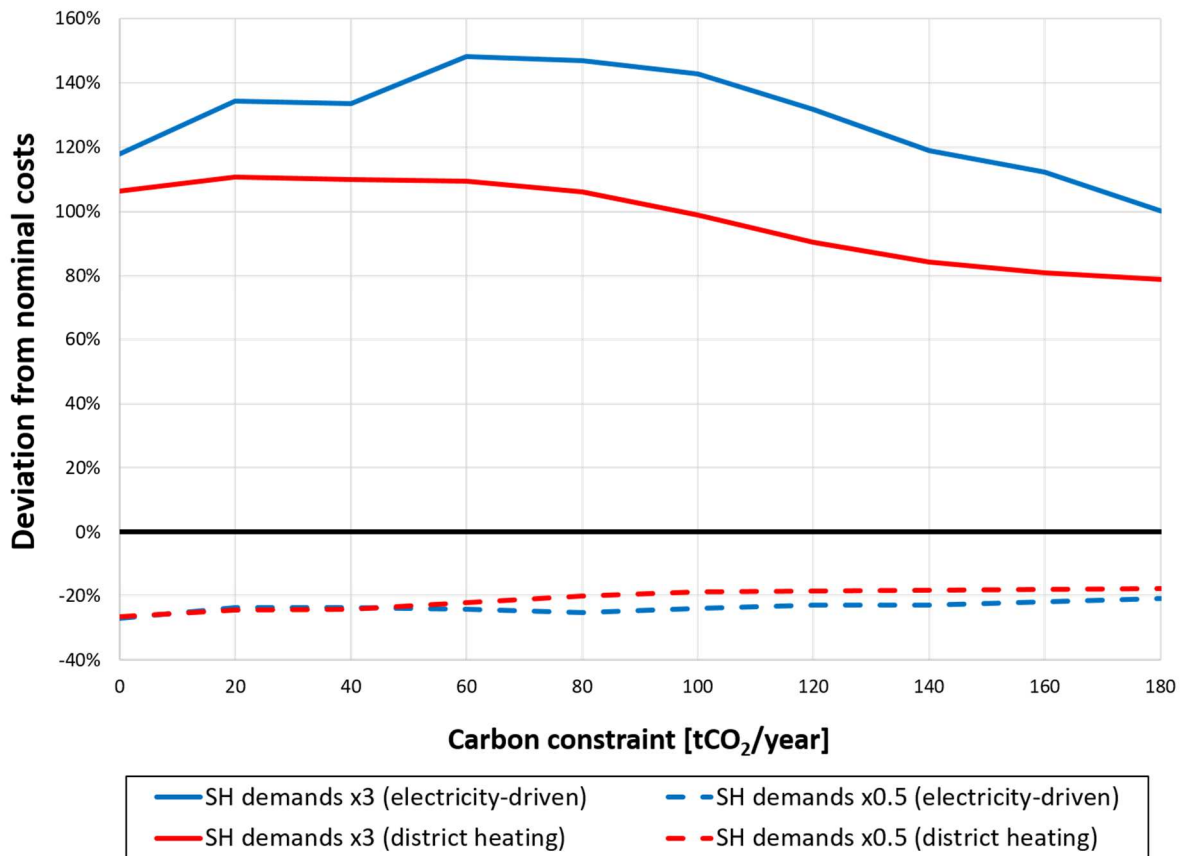


Figure 9. Sensitivity of both architectures to variations in space heating demands.

When considering a higher SH consumption, both architectures feature increased investment costs in the heat pump, as well as increased electricity purchase costs. In the district heating case, there is also a significant increase in the share of solar thermal energy and thermal storage for lowest carbon constraints: this choice allows reducing the sizing of the heat pump and PV panels, which would become very costly when trying to address such a high SH demand on renewable energy only.

When considering a lower SH consumption, both architectures feature slightly decreased investment costs in the heat pump, as well as electricity purchase costs. However, this decrease is limited, since the resulting energy consumption is dominated by DHW and specific electricity needs. In the District Heating architecture, it can be noted that low carbon emission levels (20 tCO<sub>2</sub>/y) can be obtained without significantly increasing the project costs, and only adding PV panels and storages to the systems.

Although more detailed analysis would be necessary, these results suggest that transitioning from the current average building stock to a highly efficient building stock would be more flexible when considering a district heating architecture. In particular, it is possible to attain low emission levels even for the current build stock using solar thermal energy, which could be progressively replaced by PV panels and electric storages when building performance increase and/or carbon emission constraints become stronger.

## 4. CONCLUSION AND PERSPECTIVES

Systems for providing heat at a residential level are evolving towards centralized production of heat, the implementation of district heating, and a multi-source layout. These new centralized systems rely on different equipment, at a bigger scale. Therefore, one could think that they do not have the same uncertainties. This article analyzes the robustness of a centralized architecture for a district heating system, and compares it to that of a decentralized architecture. The decentralized architecture relies on the national electric grid, plus a building-by-building possible installation of PV panels, heat pumps, electric batteries and thermal storage. The centralized architecture considers these same technologies, but sized for the whole district and backed up by a district heating network. In addition, it considers solar thermal collectors, a gas boiler plant, a biomass-fired cogeneration plant, and thermocline storage as additional means of energy management. The following conclusions were drawn:

- Constraints on the maximum allowed carbon dioxide emissions were the most influential parameter on the system design. The objective of minimizing these emissions comes at the price of increasing total costs exponentially. In addition, it requires the use of renewable sources, namely solar panels in substitution of gas and electricity from the grid.
- The decentralized, electricity-driven architecture is more sensitive to carbon constraints than the centralized, multi-source district heating architecture. When going from unconstrained to zero-emission scenarios, total costs increased by more than 9-fold for the former, versus 4-fold for the latter.
- At scenarios with very low emissions, the district heating architecture relies more on thermal storage than the electricity-driven architecture. Reasons are lower equipment costs and lesser heat losses at larger scales, plus the possibility of seasonal storage. Peak load shaving thanks to mutualizing the units played a role, too. On the other hand, the electricity-driven architecture relies on small storage tanks to reduce DHW peaks.
- The electricity-driven architecture is more sensitive than the district heating architecture to the *COP* of the heat pump. Equal variations in *COP* (+/- 33%) led to greater deviations in total costs for the former (+35% / -15%) than for the latter (< 6%).
- The inclusion of solar thermal collectors in addition to photovoltaic panels is relevant at district scale. Especially at low-emissions scenarios, the investments on ST collectors (+ thermal storage) and PV panels (+ electric storage) are balanced. This is because an optimizer can find the sizes that maximize the self-production and -consumption indices for both technologies. This illustrates the importance of accounting for the operating phase when optimizing the choice of technologies and their sizes.
- Carbon taxes seem to have an impact only on the total cost of the system, and not on its optimal architecture. Furthermore, the economic impact is rather negligible, at least in the French context in which grid electricity is both affordable and low-carbon.

The authors have two main perspectives for this study case. The first one consists in model predictive control through multi-temporal horizons, conversely to the yearly horizon used for this article. Multi-horizons are necessary for achieving realistic optimizations, since perfect yearly predictions are not possible for energy demands, fuel prices or solar irradiation, among other variables. In the multi-temporal horizon approach, the farthest possible prediction will be 24 hours. This horizon will be updated at every time step, and consequently

the optimal management too. This should lead to different results with respect to a yearly horizon.

The second perspective is to account for the buildings' thermal inertia for better optimizations. This approach requires a specific module for thermal simulation of the buildings. Such module will be integrated using a co-simulation approach.

## ACKNOWLEDGEMENT

The authors are grateful to the Institut Carnot Energies du Futur for their financial support through the DISTRISIM project ("Gestion Multi-vecteur de la Demande, une approche par Co-Simulation").

## CRedit Authorship Statement

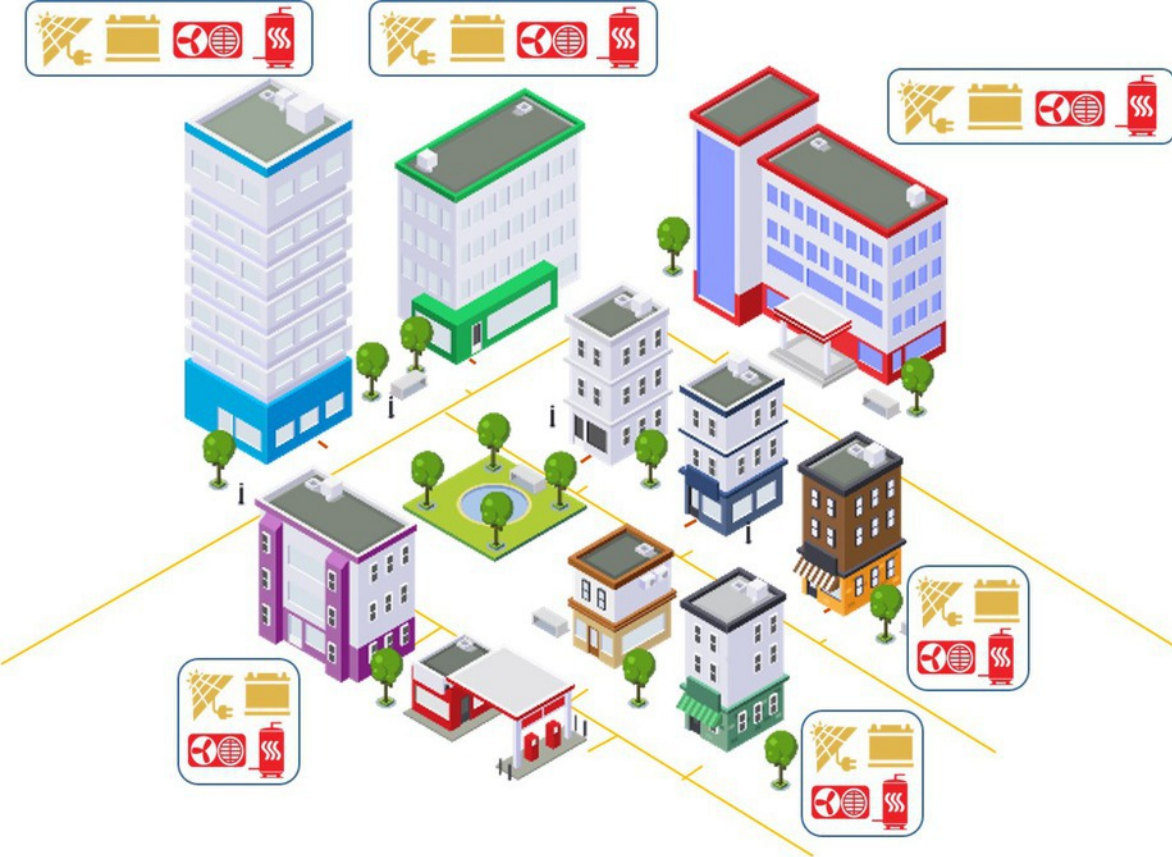
**Jaume Fitó:** Data curation, Formal analysis, Investigation, Methodology, Software, Visualization, Writing – original draft, Writing – review & editing. **Mathieu Vallée:** Conceptualization, Data curation, Formal analysis, Funding acquisition, Investigation, Methodology, Project administration, Resources, Software, Supervision, Validation, Writing – original draft, Writing – review & editing. **Alain Ruby:** Conceptualization, Data curation, Formal analysis, Funding acquisition, Methodology, Resources, Software, Supervision, Validation. **Etienne Cuisinier:** Data curation, Investigation, Resources, Software, Writing – original draft.

## REFERENCES

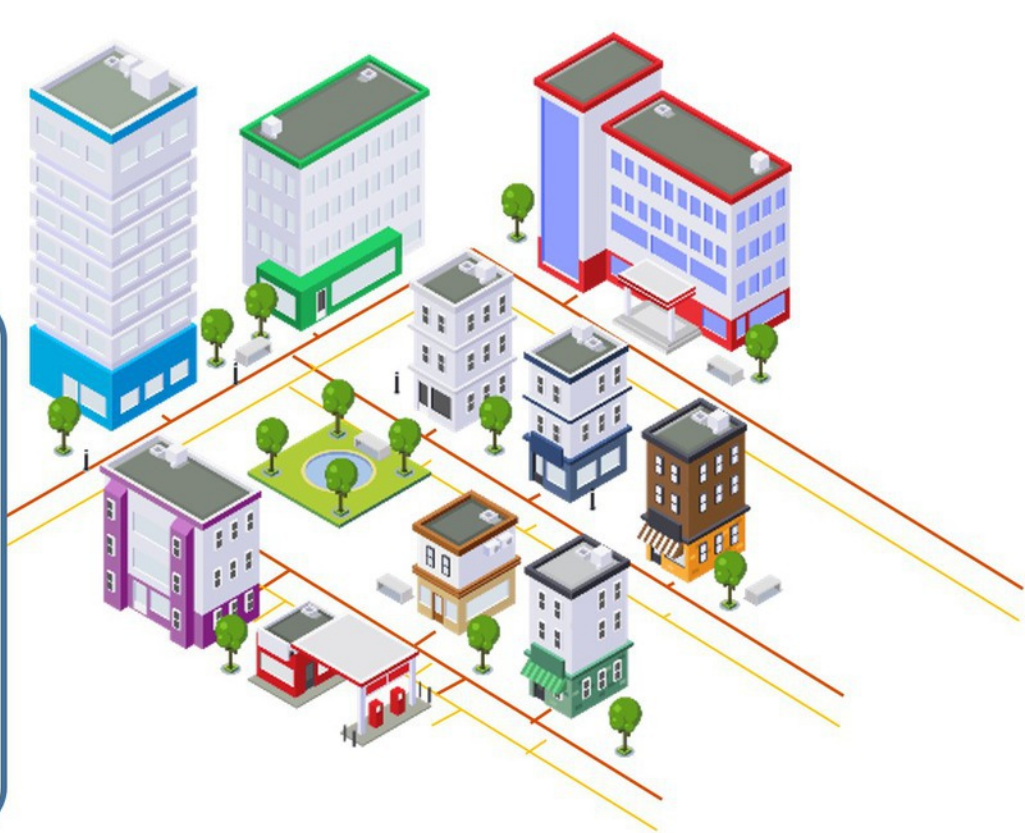
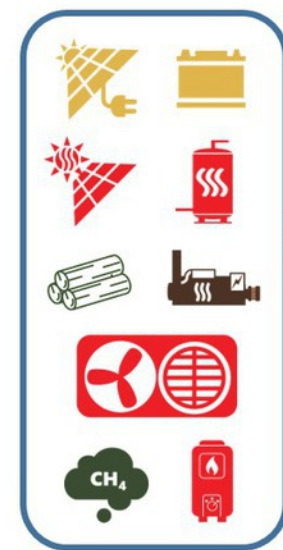
- [1] D. Ürge-Vorsatz, L. F. Cabeza, S. Serrano, C. Barreneche, and K. Petrichenko, "Heating and cooling energy trends and drivers in buildings," *Renew. Sustain. Energy Rev.*, vol. 41, pp. 85–98, 2015, doi: 10.1016/j.rser.2014.08.039.
- [2] RTE, "Energy pathways 2050 - Key results. October 2021."
- [3] A. Clerjon and F. Perdu, "Matching intermittency and electricity storage characteristics through time scale analysis: an energy return on investment comparison," *Energy Environ. Sci.*, vol. 12, no. 2, pp. 693–705, 2019.
- [4] A. Vandermeulen, B. van der Heijde, and L. Helsen, "Controlling district heating and cooling networks to unlock flexibility: A review," *Energy*, vol. 151, pp. 103–115, 2018, doi: 10.1016/j.energy.2018.03.034.
- [5] P. Mancarella, "MES (multi-energy systems): An overview of concepts and evaluation models," *Energy*, vol. 65, pp. 1–17, 2014, doi: 10.1016/j.energy.2013.10.041.
- [6] H. Lund, P. A. Østergaard, D. Connolly, and B. V. Mathiesen, "Smart energy and smart energy systems," *Energy*, vol. 137, pp. 556–565, 2017, doi: 10.1016/j.energy.2017.05.123.
- [7] A. Arabkoohsar, A. Behzadi, and A. S. Alsagri, "Techno-economic analysis and multi-objective optimization of a novel solar-based building energy system; An effort to reach the true meaning of zero-energy buildings," *Energy Convers. Manag.*, vol. 232, no. November 2020, p. 113858, 2021, doi: 10.1016/j.enconman.2021.113858.
- [8] S. Paiho and F. Reda, "Towards next generation district heating in Finland," *Renew. Sustain. Energy Rev.*, vol. 65, pp. 915–924, 2016, doi: 10.1016/j.rser.2016.07.049.
- [9] Y. Su, P. Hiltunen, S. Syri, and D. Khatiwada, "Decarbonization strategies of Helsinki metropolitan area district heat companies," *Renew. Sustain. Energy Rev.*, vol. 160, no. January, p. 112274, 2022, doi: 10.1016/j.rser.2022.112274.
- [10] E. Mäki, L. Kannari, I. Hannula, and J. Shemeikka, "Decarbonization of a district heating system with a combination of solar heat and bioenergy: A techno-economic case study in the Northern European context," *Renew. Energy*, vol. 175, pp. 1174–1199, 2021, doi: 10.1016/j.renene.2021.04.116.
- [11] P. Sorknæs, P. A. Østergaard, J. Z. Thellufsen, H. Lund, S. Nielsen, S. Djørup, K. Sperling, "The benefits of 4th generation district heating in a 100% renewable energy system," *Energy*, vol. 213, p. 119030, 2020, doi: 10.1016/j.energy.2020.119030.
- [12] K. Johansen and S. Werner, "Something is sustainable in the state of Denmark: A review of the Danish district heating sector," *Renew. Sustain. Energy Rev.*, vol. 158, no. December 2021, p. 112117, 2022, doi: 10.1016/j.rser.2022.112117.
- [13] L. Di Lucia and K. Ericsson, "Low-carbon district heating in Sweden - Examining a successful energy transition," *Energy Res. Soc. Sci.*, vol. 4, no. C, pp. 10–20, 2014, doi: 10.1016/j.erss.2014.08.005.

- [14] K. Sernhed, K. Lygnerud, and S. Werner, "Synthesis of recent Swedish district heating research," *Energy*, vol. 151, pp. 126–132, 2018, doi: 10.1016/j.energy.2018.03.028.
- [15] E. Latõšov, S. Umbleja, and A. Volkova, "Promoting efficient district heating in Estonia," *Util. Policy*, vol. 75, no. December 2021, 2022, doi: 10.1016/j.jup.2021.101332.
- [16] R. Jonynas, E. Puida, R. Poškas, L. Paukštaitis, H. Jouhara, J. Gudzinskas, G. Miliuskas, V. Lukoševičius, "Renewables for district heating: The case of Lithuania," *Energy*, vol. 211, 2020, doi: 10.1016/j.energy.2020.119064.
- [17] N. Aste, P. Caputo, C. Del Pero, G. Ferla, H. E. Huerto-Cardenas, F. Leonforte, A. Miglioli, "A renewable energy scenario for a new low carbon settlement in northern Italy: Biomass district heating coupled with heat pump and solar photovoltaic system," *Energy*, vol. 206, 2020, doi: 10.1016/j.energy.2020.118091.
- [18] C. B. Heendeniya, A. Sumper, and U. Eicker, "The multi-energy system co-planning of nearly zero-energy districts – Status-quo and future research potential," *Appl. Energy*, vol. 267, no. November 2019, p. 114953, 2020, doi: 10.1016/j.apenergy.2020.114953.
- [19] L. M. P. Ghilardi, A. F. Castelli, L. Moretti, M. Morini, and E. Martelli, "Co-optimization of multi-energy system operation, district heating/cooling network and thermal comfort management for buildings," *Appl. Energy*, vol. 302, no. March, p. 117480, 2021, doi: 10.1016/j.apenergy.2021.117480.
- [20] S. Xie, J. Zheng, Z. Hu, J. Wang, and Y. Chen, "Urban multi-energy network optimization: An enhanced model using a two-stage bound-tightening approach," *Appl. Energy*, vol. 277, no. July, p. 115577, 2020, doi: 10.1016/j.apenergy.2020.115577.
- [21] J. Naughton, H. Wang, S. Riaz, M. Cantoni, and P. Mancarella, "Optimization of multi-energy virtual power plants for providing multiple market and local network services," *Electr. Power Syst. Res.*, vol. 189, no. October 2019, p. 106775, 2020, doi: 10.1016/j.epsr.2020.106775.
- [22] J. F. Marquant, R. Evins, L. A. Bollinger, and J. Carmeliet, "A holarchic approach for multi-scale distributed energy system optimisation," *Appl. Energy*, vol. 208, no. May, pp. 935–953, 2017, doi: 10.1016/j.apenergy.2017.09.057.
- [23] G. Mavromatidis and I. Petkov, "MANGO: A novel optimization model for the long-term, multi-stage planning of decentralized multi-energy systems," *Appl. Energy*, vol. 288, no. February, p. 116585, 2021, doi: 10.1016/j.apenergy.2021.116585.
- [24] R. Jing, M. Wang, Z. Zhang, X. Wang, N. Li, N. Shah, Y. Zhao, "Distributed or centralized? Designing district-level urban energy systems by a hierarchical approach considering demand uncertainties," *Appl. Energy*, vol. 252, no. June, p. 113424, 2019, doi: 10.1016/j.apenergy.2019.113424.
- [25] P. Gabrielli, F. Furer, G. Mavromatidis, and M. Mazzotti, "Robust and optimal design of multi-energy systems with seasonal storage through uncertainty analysis," *Appl. Energy*, vol. 238, no. December 2018, pp. 1192–1210, 2019, doi: 10.1016/j.apenergy.2019.01.064.
- [26] F. Si, Y. Han, Q. Zhao, and J. Wang, "Cost-effective operation of the urban energy system with variable supply and demand via coordination of multi-energy flows," *Energy*, vol. 203, p. 117827, 2020, doi: 10.1016/j.energy.2020.117827.
- [27] G. Coccia, A. Mugnini, F. Polonara, and A. Arteconi, "Artificial-neural-network-based model predictive control to exploit energy flexibility in multi-energy systems comprising district cooling," *Energy*, vol. 222, p. 119958, 2021, doi: 10.1016/j.energy.2021.119958.
- [28] M. Dahl, A. Brun, and G. B. Andresen, "Cost sensitivity of optimal sector-coupled district heating production systems," *Energy*, vol. 166, pp. 624–636, 2019, doi: 10.1016/j.energy.2018.10.044.
- [29] C. You and J. Kim, "Optimal design and global sensitivity analysis of a 100% renewable energy sources based smart energy network for electrified and hydrogen cities," *Energy Convers. Manag.*, vol. 223, no. July, p. 113252, 2020, doi: 10.1016/j.enconman.2020.113252.
- [30] M. Zirak, V. Weiler, M. Hein, and U. Eicker, "Urban models enrichment for energy applications: Challenges in energy simulation using different data sources for building age information," *Energy*, vol. 190, p. 116292, 2020, doi: 10.1016/j.energy.2019.116292.
- [31] V. Verda and F. Colella, "Primary energy savings through thermal storage in district heating networks," *Energy*, vol. 36, no. 7, pp. 4278–4286, 2011, doi: 10.1016/j.energy.2011.04.015.
- [32] J. Wang, Y. Zhou, X. Zhang, Z. Ma, Y. Gao, B. Liu, Y. Qin, "Robust multi-objective optimization with life cycle assessment of hybrid solar combined cooling, heating and power system," *Energy Convers. Manag.*, vol. 232, no. November 2020, p. 113868, 2021, doi: 10.1016/j.enconman.2021.113868.
- [33] C. Pajot, N. Artiges, B. Delinchant, S. Rouchier, F. Wurtz, and Y. Maréchal, "An approach to study district thermal flexibility using generative modeling from existing data," *Energies*, vol. 12, no. 19, pp. 1–22, 2019, doi: 10.3390/en12193632.
- [34] J. Fitó, S. Hodencq, J. Ramousse, F. Wurtz, B. Stutz, F. Debray, B. Vincent, "Energy- and exergy-based optimal designs of a low-temperature industrial waste heat recovery system in district heating," *Energy Convers. Manag.*, vol. 211, no. December 2019, p. Article number 112753, 2020, doi: 10.1016/j.enconman.2020.112753.
- [35] E. Cuisinier, C. Bourasseau, A. Ruby, P. Lemaire, and B. Penz, "Impact of operational modelling choices on techno-economic modelling of local energy systems. Article in preparation," 2021.
- [36] S. Mouret, M. Chammas, P. Attard, J. De Bucy, H. Lochmann, L. Le Gars, L. Payen, H. Lesueur, "Étude de valorisation du stockage thermique et du power-to-heat," ADEME/ATTE, France, 2016.
- [37] T. Schmidt, D. Mangold, and H. Müller-Steinhagen, "Central solar heating plants with seasonal storage in Germany,"

- Sol. Energy*, vol. 76, no. 1–3, pp. 165–174, 2004, doi: 10.1016/j.solener.2003.07.025.
- [38] A. Bejan, G. Tsatsaronis, and M. Moran, *Thermal Design and Optimization*, 1st ed. Canada: John Wiley & Sons, 1996.
- [39] “Eurostat Data Browser: Price of electricity per type of user.” <https://ec.europa.eu/eurostat/databrowser/view/ten00117/default/table?lang=fr> (accessed Apr. 20, 2021).
- [40] Danish Energy Agency and Energinet, “Technology Data - Energy Plants for Electricity and District heating generation,” no. 36, p. 414, 2020.
- [41] L. Cadiou, M. Allain, M. Descat, G. Perrin, R. Roy, L. Dagallier, J. Purdue, G. Planchot, S. Cousin, C. Fisher, H. Lhoir, O. Conte, P. Laugier, P. Hourcade, P. Cameijo, B. Khebchache, D. Canal, “ADEME – Les réseaux de chaleur et de froid – état des lieux de la filière. [Technical report],” 2019.
- [42] N. Ahmed, K. E. Elfeky, L. Lu, and Q. W. Wang, “Thermal and economic evaluation of thermocline combined sensible-latent heat thermal energy storage system for medium temperature applications,” *Energy Convers. Manag.*, vol. 189, no. March, pp. 14–23, 2019, doi: 10.1016/j.enconman.2019.03.040.
- [43] “Eurostat Data Browser: Price of gas per type of user.” <https://ec.europa.eu/eurostat/databrowser/view/ten00118/default/table?lang=fr> (accessed Jul. 28, 2021).
- [44] G. T. Armstrong and T. L. Jobe, “Heating Values of Natural Gas and Its Components,” *Tech. Rep.*, no. August, p. 172, 1982.
- [45] N. Lamaison, S. Collette, M. Vallée, and R. Bavière, “Storage influence in a combined biomass and power-to-heat district heating production plant,” *Energy*, vol. 186, 2019, doi: 10.1016/j.energy.2019.07.044.
- [46] “Biogenic carbon dioxide emissions,” *The French Agency for Ecological Transition (ADEME)*, 2015. [https://bilans-ges.ademe.fr/documentation/UPLOAD\\_DOC\\_FR/index.htm?co2\\_biogenique.htm](https://bilans-ges.ademe.fr/documentation/UPLOAD_DOC_FR/index.htm?co2_biogenique.htm) (accessed Sep. 05, 2021).
- [47] R. McKenna, L. Hofmann, M. Kleinebrahm, and W. Fichtner, “A stochastic multi-energy simulation model for UK residential buildings,” *Energy Build.*, vol. 168, pp. 470–489, 2018, doi: 10.1016/j.enbuild.2018.02.051.
- [48] E. McKenna and M. Thomson, “High-resolution stochastic integrated thermal-electrical domestic demand model,” *Appl. Energy*, vol. 165, pp. 445–461, 2016, doi: 10.1016/j.apenergy.2015.12.089.
- [49] E. McKenna, M. Krawczynski, and M. Thomson, “Four-state domestic building occupancy model for energy demand simulations,” *Energy Build.*, vol. 96, pp. 30–39, 2015, doi: 10.1016/j.enbuild.2015.03.013.
- [50] UK Office for National Statistics [ONS], *The United Kingdom 2005 Time Use Survey*, no. August. 2006. [Online]. Available: <http://www.ons.gov.uk/ons/rel/lifestyles/time-use/2005-edition/index.html>
- [51] E. Cuisinier, C. Bourasseau, A. Ruby, P. Lemaire, and B. Penz, “Techno-economic planning of local energy systems through optimization models: a survey of current methods,” *Int. J. Energy Res.*, vol. 45, no. 4, pp. 4888–4931, 2021, doi: 10.1002/er.6208.
- [52] E. Cuisinier, “Techno-economic modelling and optimisation methods for the planning of multi-energy systems. Doctoral Thesis. <http://theses.fr/s215019>,” University of Grenoble Alpes, France, 2021. [Online]. Available: <http://theses.fr/s215019>
- [53] É. Cuisinier, P. Lemaire, B. Penz, A. Ruby, and C. Bourasseau, “New rolling horizon optimization approaches to balance short-term and long-term decisions: An application to energy planning,” *Energy*, vol. 245, p. 122773, 2022, doi: 10.1016/j.energy.2021.122773.
- [54] “N. Lamaison. Personal communication, Laboratory of Energy Systems and Territory (France), 30/09/2021.”.
- [55] “Average energy consumption for residential space heating in France,” *The French Agency for Ecological Transition (ADEME)*, 2015. [https://www.bilans-ges.ademe.fr/documentation/UPLOAD\\_DOC\\_FR/index.htm?chauffage.htm](https://www.bilans-ges.ademe.fr/documentation/UPLOAD_DOC_FR/index.htm?chauffage.htm) (accessed Sep. 05, 2021).
- [56] “ENTSOE Transparency platform, ‘Day Ahead Prices (hourly data for 2018 on bidding zone FR),’” 2018.
- [57] “EUROSTAT, ‘Electricity prices by type of user [TEN00117].’”



***(Electricity-driven architecture)***



***(District heating architecture)***

